PHYSICAL REVIEW B **85**, 041402(R) (2012)

Effect of the band structure topology on the minimal conductivity for bilayer graphene with symmetry breaking

Gyula Dávid,[1] Péter Rakyta,[2] László Oroszlány,[2] and József Cserti[2]
[1]*Department of Atomic Physics, Eötvös University, Pázmány Péter sétány 1/A, H-1117 Budapest, Hungary*
[2]*Department of Physics of Complex Systems, Eötvös University, Pázmány Péter sétány 1/A, H-1117 Budapest, Hungary*
(Received 14 December 2011; published 6 January 2012)

Using the Kubo formula we develop a general and simple expression for the minimal conductivity in systems described by a 2×2 Hamiltonian. As an application we derive an analytical expression for the minimal conductivity tensor of bilayer graphene as a function of a complex parameter w related to recently proposed symmetry breaking mechanisms resulting from electron-electron interaction or strain applied to the sample. The number of Dirac points changes with varying parameter w, and this directly affects the minimal conductivity. Our analytic expression is confirmed using an independent calculation based on the Landauer approach, and we find remarkably good agreement between the two methods. We demonstrate that the minimal conductivity is very sensitive to the change of the parameter w and the orientation of the electrodes with respect to the sample. Our results show that the minimal conductivity is closely related to the topology of the low-energy band structure.

DOI: 10.1103/PhysRevB.85.041402 PACS number(s): 81.05.ue, 72.10.Bg, 72.80.Vp, 73.23.Ad

Introduction. After the first quantum Hall measurement on graphene,[1,2] the physics of graphene has become one of the leading research fields in physics. The bilayer graphene has been studied first experimentally by Novoselov *et al.*[3] and theoretically by McCann and Fal'ko.[4] Recent observations[5,6] indicate that in bilayer graphene spontaneous symmetry breaking may arise from electron-electron Coulomb interactions. The occurence of such broken-symmetry states generates more attention to the topological changes in the Fermi surface in high-quality suspended bilayer graphene devices. Lemonik *et al.* studied the spontaneous symmetry breaking and Lifshitz transition in bilayer graphene.[7] Spontaneous inversion symmetry breaking in graphene bilayers has also been investigated by Zhang *et al.*[8] Vafek and Yang applied the renormalization group approach to study the many-body instability of Coulomb interacting bilayer graphene.[9] Nandkishore and Levitov[10] and Gorbar *et al.*[11] studied the competition between different ordered states in bilayer graphene. Spontaneous symmetry breaking in two-dimensional electronic systems with a quadratic band crossing was studied by Sun *et al.*[12] The quantum theory of a nematic Fermi fluid has been proposed by Oganesyan *et al.*[13]

The symmetry breaking induced by the electron-electron interaction in bilayer graphene can be described adequately by the Hamiltonian suggested by Lemonik *et al.*[7] Very recently, the same form of the Hamiltonian has been derived by Mucha-Kruczyński, Aleiner, and Fal'ko for electrons in strained bilayer graphene.[14] They studied the band structure topology and Landau-level spectrum for strained bilayer graphene. The Hamiltonian depends on a complex parameter w and its change causes a transition in the electronic band structure. However, the effect of the symmetry breaking on the minimal conductivity $\sigma^{\min}$, the conductivity measured at zero frequency, at zero temperature, and zero Fermi energy is an open question. Our main aim in this Rapid Communication is to address this issue.

The low-energy Fermi surface of bilayer graphene is dominated by the effect of trigonal warping, first shown by McCann and Fal'ko.[4] At very low energies, namely, below the Lifshitz energy, trigonal warping results in a breaking of the constant energy lines into four pockets. Thus, by varying the Fermi energy, the Fermi surface undergoes a change in topology at the Lifshitz energy. The Lifshitz energy is typically of order of 1 meV.[4,15] This is one type of topological phase transition in bilayer graphene. However, the topology of the Fermi surface can also be changed by symmetry breaking when the position of the pockets and even the number of pockets can be altered (for more details and figures on the topology of the band structures, see Ref. 14). In this Rapid Communication we consider the effect of the latter scenario on the minimal conductivity $\sigma^{\min}$.

Without trigonal warping, in Ref. 16 it was found that $\sigma^{\min} = 8\sigma_0$, where $\sigma_0 = e^2/(\pi h)$. This later was confirmed by Snyman and Beenakker[17] by using the Landauer approach. Actually, the calculated minimal conductivity can take nonuniversal values depending on the order of the dc limit and the integration over energies as shown by Ziegler.[18] The importance of the order of the frequency and the temperature limit was pointed out by Ryu *et al.*[19] Trushin *et al.* showed that electron-hole puddle formation is not a necessary condition for finite conductivity in bilayer graphene at zero average carrier density.[20] Culcer and Winkler studied the role of the external gates and transport in biased bilayer graphene by using the density operator formalism and quantum Liouville equation.[21] From the self-consistent Born approximation, Koshino and Ando[22] found that in the strong-disorder regime $\sigma^{\min} = 8\sigma_0$, while in the weak-disorder regime $\sigma^{\min} = 24\sigma_0$. In Ref. 23 the role of trigonal warping was studied, and it was shown that the contributions of the four pockets to the minimal conductivity gives $\sigma^{\min} = 24\sigma_0$. Moghaddam and Zareyan showed that the minimal conductivity of graphene bilayers is anisotropic with respect to the orientation of the connected electrodes when the trigonal warping is taken into account.[24]

Here we calculate the minimal conductivity of bilayer graphene as a function of the parameter w related to the symmetry breaking of the system. We find that the change in this parameter can dramatically affect the minimal conductivity. Starting from the Kubo formula, we develop a general and

simple method to find the minimal conductivity for a wide class of Hamiltonians. By using this general approach we derive an analytical expression for the conductivity tensor in bilayer graphene with symmetry breaking by a complex parameter w. As a self-check we performed numerical calculations based on the Landauer formula, and the agreement is very good. Our analysis of the minimal conductivity presented in this paper was inspired by a recent experiment[25] and insightful discussions with Novoselov.

General approach. To calculate the conductivity of various two-dimensional electronic systems with electron-hole symmetry, we consider a general model Hamiltonian:

$$H(\mathbf{p}) = \mathbf{\Omega}(\mathbf{p})\boldsymbol{\tau}, \tag{1}$$

where $\mathbf{\Omega}(\mathbf{p})$ is an arbitrary differentiable function of the momentum $\mathbf{p} = (p_x, p_y)$ and $\boldsymbol{\tau} = (\tau_x, \tau_y, \tau_z)$ is a vector formed from the Pauli matrices and acts on the pseudospin space. Specifically, the Hamiltonian for bilayer graphene including symmetry breaking has this form with

$$\mathbf{\Omega}(\mathbf{p}) = -\varepsilon_{\mathrm{L}} \begin{pmatrix} p_x^2 - p_y^2 - 2p_x - \mathrm{Re}(w) \\ 2p_y(p_x + 1) + \mathrm{Im}(w) \\ 0 \end{pmatrix}, \tag{2}$$

valid for the valley $\mathbf{K}$. Here $\varepsilon_{\mathrm{L}} = m v_3^2/2$ is the Lifshitz energy (where m and v_3 are given in Ref. 4), and the dimensionless momenta p_x and p_y are in units of $m v_3$. Finally, w is generally a dimensionless complex parameter (independent of $\mathbf{p}$) and can be originated from the electron-electron interaction[7] and/or from the applied strain[14] and/or from the slide of the layer.[14,26] The topology of the band structure for Hamiltonian (1) in terms of the parameter w have been extensively studied in the above references.

To find the conductivity for clean and bulk systems, we start from the general Kubo formula presented in Ref. 23 (derived from the form given by Ryu *et al.*[19]). The minimal dc conductivity (at zero frequency, at zero temperature, and at zero Fermi energy) is given by

$$\sigma_{lm}^{\min} = n_d \frac{2e^2}{h} \lim_{\eta\to 0} I_{lm}(\eta), \tag{3a}$$

where

$$I_{lm}(\eta) = \eta^2 \int \frac{d^2\mathbf{k}}{(2\pi)^2} \mathrm{Tr}\, T_{lm}(\mathbf{k},\eta), \tag{3b}$$

$$T_{lm}(\mathbf{k},\eta) = [\eta^2 + H^2(\mathbf{k})]^{-1} \frac{\partial H(\mathbf{k})}{\partial k_l} \times [\eta^2 + H^2(\mathbf{k})]^{-1} \frac{\partial H(\mathbf{k})}{\partial k_m}, \tag{3c}$$

and $\mathbf{p} = \hbar\mathbf{k}$, $l,m = x,y$, and n_d is the degeneracy (for bilayer graphene $n_d = n_s n_v$, where $n_s = 2$ is the spin degeneracy and $n_v = 2$ is the valley degeneracy corresponding to the valleys $\mathbf{K}$ and $\mathbf{K}'$). The trace is taken over the spinor indices. Without the limit $\eta \to 0$ in Eq. (3a) the parameter η can be interpreted physically as a finite inverse lifetime induced by impurities.

The eigenvalues of the Hamiltonian (1) are $E(\mathbf{k}) = \pm|\mathbf{\Omega}(\mathbf{k})|$. The operator inverse in Eq. (3c) can be written as $[\eta^2 + H^2(\mathbf{k})]^{-1} = I_2/[\eta^2 + E^2(\mathbf{k})]$, where I_2 is the 2×2 unit matrix. Hence, the main contribution of the integrand in Eq. (3b) comes from the vicinity of the zeros of the energy eigenvalues. The real solutions of $E(\mathbf{k}) = 0$ are denoted by $\mathbf{k}^{(s)}$, where $s = 1,\ldots,n_{\mathrm{D}}$ and n_{D} is the number of zeros (for bilayer graphene $n_{\mathrm{D}} = 2,3,4$ depending on the parameter w). Expanding $E^2(\mathbf{k})$ around one of the zeros $\mathbf{k}^{(s)}$, i.e., for fixed s the denominator becomes a polynomial of $\mathbf{q}$, where $\mathbf{q} = \mathbf{k} - \mathbf{k}^{(s)}$. If the energy dispersion $E(\mathbf{k})$ at the point $\mathbf{k}^{(s)}$ forms a Dirac cone, then the leading term of the expansion is quadratic in $\mathbf{q}$ [otherwise one needs to expand $E^2(\mathbf{k})$ beyond the quadratic terms in $\mathbf{q}$], and can be written as $E^2(\mathbf{q}) = \sum_{i,j} M_{ij} q_i q_j$, where the matrix M is positive semidefinite and $i,j = 1,2$. For the Hamiltonian (1) one finds

$$M_{ij} = \sum_{l=1}^{3} \frac{\partial \Omega_l}{\partial k_i} \frac{\partial \Omega_l}{\partial k_j}, \tag{4}$$

where the derivations are evaluated at $\mathbf{k} = \mathbf{k}^{(s)}$. Moreover, we find that $\mathrm{Tr}[\frac{\partial H(\mathbf{k})}{\partial k_l}\frac{\partial H(\mathbf{k})}{\partial k_m}] = 2M_{lm}$ and $T_{lm}(\mathbf{q},\eta) = 2M_{lm}/(\eta^2 + \sum_{i,j} M_{ij} q_i q_j)^2$.

Now substituting this expression into (3b) and rescaling the wave number $\mathbf{q}$ as $\mathbf{q} = \eta\mathbf{q}'$, the integral I_{lm} becomes *independent* of η, and reads

$$I_{lm} = 2M_{lm} \int \frac{d^2\mathbf{q}'}{(2\pi)^2} \frac{1}{\left(1 + \sum_{i,j} M_{ij} q_i' q_j'\right)^2}. \tag{5}$$

Note that for the limit $\eta \to 0$ the main contribution in the integral I_{lm} comes from the vicinity of each Dirac point; therefore, the integral over $\mathbf{q}'$ can be extended to infinity.

If the determinant of the matrix M at $\mathbf{k}^{(s)}$ is zero, then the integral is divergent. For a finite determinant of M the integral in Eq. (5), i.e., the contribution to the integral (3b) over the vicinity of $\mathbf{k}^{(s)}$ can be performed analytically and it becomes $I_{lm}^{(s)} = \frac{1}{2\pi} M_{lm}^{(s)}/\sqrt{\det M^{(s)}}$. Here $M_{lm}^{(s)}$ denotes the matrix defined in Eq. (4) evaluated at $\mathbf{k} = \mathbf{k}^{(s)}$.

Then using Eq. (3a) the minimal conductivity is the sum of the contributions from each Dirac cones at $\mathbf{k}^{(s)}$:

$$\sigma_{lm}^{\min} = n_d \sigma_0 \sum_{s=1}^{n_{\mathrm{D}}} \frac{M_{lm}^{(s)}}{\sqrt{\det M^{(s)}}}. \tag{6}$$

This universal procedure to find the minimal conductivity for clean systems can be applied for all Hamiltonians given by Eq. (1) except for cases when the determinant of the matrix M is zero at any of the Dirac points. In such cases, we cannot derive an universal and η independent expression for the minimal conductivity, and one needs to evaluate Eq. (3) numerically for finite η. However, if the value of η in Eq. (3) is less than the energy scale for which the quadratic expansion of $E^2(\mathbf{k})$ is valid, then our expression (6) gives the same result as that obtained numerically from Eq. (3). In such cases the minimal conductivity is independent of the value of η, i.e., the microscopic details of the systems.

Applications. We now apply our method for calculating the minimal conductivity in different models of bilayer graphene.

(i) The simplest case is when the trigonal warping is absent, i.e., the linear term in momentum is missing in Eq. (2). Then we find that $\boldsymbol{\sigma}^{\min}(w) = 8\sigma_0 I_2$ and is independent of w and η.

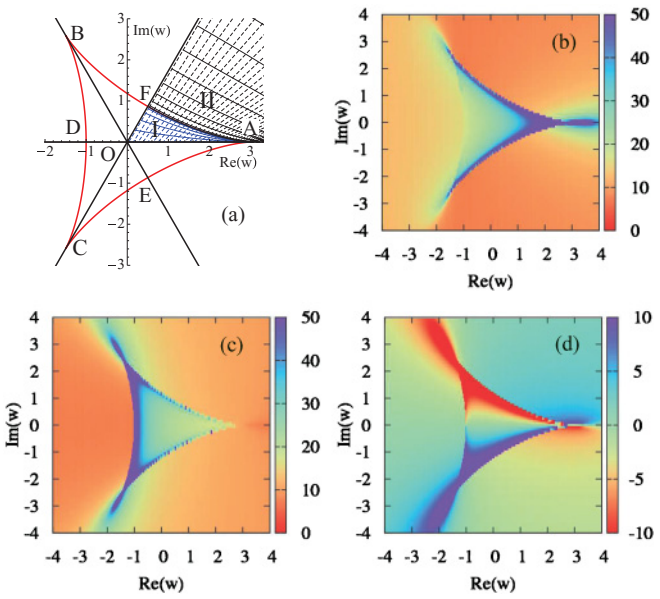

FIG. 1. (Color online) (a) The topologically distinct regions of the complex w plane. Inside (outside) of the triangular curve ABC given by $w_\triangle$ (red/gray solid line) there are four (two) separate Dirac cones. The dashed and solid lines in regions I and II correspond to constant parameters α and β, respectively. The components of the conductivity tensor (in units of σ_0) in the complex w plane: (b) $\sigma_{xx}(w)$, (c) $\sigma_{yy}(w)$, and (d) $\sigma_{xy}(w) = \sigma_{yx}(w)$.

(ii) Now we take into account the effect of the trigonal warping using the Hamiltonian (1) and (2). Then, it is easy to calculate the matrix M defined in Eq. (4) and we have

$$M(\mathbf{k}) = \varepsilon_{\mathrm{L}}^2 \begin{pmatrix} 1+\mathbf{k}^2-2k_x & 2k_y \\ 2k_y & 1+\mathbf{k}^2+2k_x \end{pmatrix}, \tag{7}$$

and $\det M = \varepsilon_{\mathrm{L}}^4(\mathbf{k}^2-1)^2$, where the wave number $\mathbf{k}$ is in units of $mv_3/\hbar$. Thus, the *singular points* (when $\det M = 0$) are located on a unit circle in the $\mathbf{k}$ plane. In this case the parameter w lies on the triangular curve ABC on the complex w plane shown in Fig. 1(a) [the same trianglelike curve is plotted in Fig. 3(a) in Ref. 14]. At these points two or three Dirac cones collide and annihilate each other, resulting in a topological phase transition in the energy band dispersion. There are *four* (*two*) Dirac points in the momentum plane for the parameter w lying inside (outside) of the triangular curve ABC, respectively.

In what follows it is useful to parametrize the complex parameter w in regions I and II in the following way:

$$w = e^{-i4\alpha} + 2\cos(2\beta)\, e^{i2\alpha}, \tag{8}$$

where $\alpha \in [0,\pi/3]$ and $0 < \beta < \min\{3\alpha, \pi - 3\alpha\}$ in region I, while in region II β is a pure imaginary number such that $i\beta < 0$. The triangular curve ABC in Fig. 1(a) in this parametrization reads as $w_\triangle(\alpha) = e^{-i4\alpha} + 2e^{i2\alpha}$, with $0 < \alpha \leqslant \pi$. The parameter w lying outside regions I and II can be folded back into either of these regions by a symmetry operation R belonging to the group C_{3v}. Note that if no symmetry breaking is present, then $w = 0$, which corresponds to $\alpha = \beta = \pi/6$.

Using the parametrization (8) the minimal conductivity can be obtained analytically from Eqs. (6) and (7) for the arbitrary complex parameter w (for the location of the Dirac points, see the Supplemental Material[27]). In region I we have

$$\frac{\boldsymbol{\sigma}_{\mathrm{I}}^{\min}}{8\sigma_0} = I_2 + \frac{1}{\sin\beta(\sin 3\alpha - \sin\beta)} \times \begin{pmatrix} \cos^2\alpha - \sin\beta\sin\alpha & \cos\alpha(\sin\beta - \sin\alpha) \\ \cos\alpha(\sin\beta - \sin\alpha) & \sin\alpha(\sin\beta + \sin\alpha) \end{pmatrix}, \tag{9a}$$

while in region II

$$\frac{\boldsymbol{\sigma}_{\mathrm{II}}^{\min}}{8\sigma_0} = I_2 + \frac{1}{\cos^2\beta - \cos^2 3\alpha} \times \begin{pmatrix} \cos^2 2\alpha & \sin 2\alpha\cos 2\alpha \\ \sin 2\alpha\cos 2\alpha & \sin^2 2\alpha \end{pmatrix}. \tag{9b}$$

The minimal conductivity for w lying outside regions I and II can be obtained by $\boldsymbol{\sigma}^{\min}(w) = R^{-1}\cdot\boldsymbol{\sigma}^{\min}(R\cdot w)\cdot R$, where R is a symmetry operation of the symmetry group C_{3v} (reflection or rotation of $\pm 120^\circ$) which transforms w into region I or II. Therefore, the minimal conductivity has a C_{3v} symmetry in the w plane. In Figs. 1(b)–1(d) we plotted the components of the minimal conductivity tensor [Eqs. (9)] as functions of the complex parameter w.

The eigenvalues of the conductivity tensor: $\sigma_{1,2}^{\mathrm{I}}/(8\sigma_0) = 1 + 2/[1 \pm \sqrt{1 - 4\sin\beta(\sin 3\alpha - \sin\beta)}]$ in region I and $\sigma_1^{\mathrm{II}}/(8\sigma_0) = 1$, while $\sigma_2^{\mathrm{II}}/(8\sigma_0) = 1 + 2/(\cos 2\beta - \cos 6\alpha)$ in region II. The minimal conductivity tensor $\boldsymbol{\sigma}^{\min}$ is a symmetric matrix, but generally for complex w the nondiagonal elements can be different from zero and can even be negative. Note that for $w = 0$ (without symmetry breaking) we recover our earlier results, namely, $\sigma_{xx}^{\min}(w=0) = \sigma_{yy}^{\min}(w=0) = 24\sigma_0$, and the off-diagonal elements are zero.[23]

We calculated numerically the components of the minimal conductivity tensor from (9) [or from Eqs. (6) and (7)] for complex parameter w and plotted in Figs. 1(b)–1(d), respectively. One can see from the figures that close to points $w_\triangle$ along the curve ABC, i.e., where the electronic topological transition occurs the conductivity changes dramatically. We compared our theoretical prediction (9) with that obtained numerically from (3) for finite η and found that the numerical results becomes better with decreasing η (for details see Fig. S1 in the Supplemental Material[27]). The analytical result (9) starts to deviate from the numerical calculations at some values of parameter w for which the Dirac points are close enough so that the energy corresponding to the saddle point between them becomes the same order of magnitude as the inverse lifetime η.

To confirm our analytical predictions (9) we calculated the conductance using the two-terminal Landauer formula[24,28,29] (for details of the calculation see the Supplemental Material,[27] and Ref. 30 therein). In these calculations the orientation $\mathbf{n} = (\cos\theta, \sin\theta)$ of the graphene sample with respect to the contacts is fixed (see Fig. S2 in the Supplemental Material[27]). From the conductivity tensor (9) the conductivity along the direction $\mathbf{n}$ in the two-terminal measurement is given by $\sigma_{\mathrm{Kubo}}(w,\mathbf{n}) = \mathbf{n}\cdot\boldsymbol{\sigma}(w)\cdot\mathbf{n}$.[19,31] Then these results should be compared with that obtained numerically from the Landauer

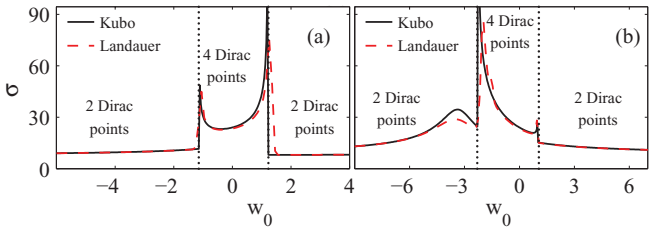

FIG. 2. (Color online) The conductivity $\sigma_{\mathrm{Kubo}}(w_0)$ (black solid line) and by numerical evaluation of the Landauer formula (red dashed line) as functions of the parameter w_0, where $w = w_0 e^{i\omega}$, and (a) $\omega = 27^\circ$, $\theta = -42^\circ$ and (b) $\omega = 57^\circ$, $\theta = 42^\circ$. The units are the same as in Fig. 1. The dotted vertical lines indicate the values of the parameter w_0 where the number of Dirac points changes.

formula. Our results are shown in Fig. 2. The complex parameter w is taken along two different lines given by the direction ω in Fig. 1(a) such that $w = w_0 e^{i\omega}$, where w_0 varies. Similarly, two electrode directions **n** are taken. As can be seen from Fig. 2, the agreement between the two approaches is very good for most of the values of w_0 (and similarly good agreements were found for other values of w and directions **n** not presented here). Note that the electronic topological transition occurs at two values of w_0, where the number of Dirac points changes from four to two (see the dotted lines in Fig. 2). Near the singular points the deviation between the numerical and analytical results arises from the fact that here the Dirac cones come closer to each other than the momentum space resolution of the numerical method dictated by the finite size of the sample in the Landauer approach. Thus, not too close to the singular points $w_\triangle$, our central result (9) well approximates the elements of the conductivity tensor for bulk and clean bilayer graphene, and it is independent of the inverse lifetime η and depends on the topology of the Fermi surface at the neutrality point.

We now comment on the experimental feasibility of measuring the minimal conductivity. On the one hand, in recent experiments[25] the bilayer graphene samples are clean enough that it is ballistic up to lengths 2–4 μm, making sense to apply the Landauer approaches and to compare with our analytical result (9) obtained from the Kubo formula. Furthermore, the temperature experimentally can be as low as $T \approx 0.25$ K ≈ 0.02 meV, i.e., its effect can be neglected in the first approximation. On the other hand, the conductivity depends very sensitively on the orientation of the sample and the values of the parameter w. Thus, these two unknown factors seem to be crucial in reproducing the measured minimal conductivity. However, with the experimental control of the direction of the electrodes, the measurement of the minimal conductivity may provide a good tool for determining the complex parameter w and exploring its origin in the electronic topological transition.

In conclusion, by using the Kubo formula we calculated analytically the minimal conductivity in bilayer graphene, taking into account the electronic topological transition. Our results are confirmed by numerical calculations of the conductivity by using the Landauer approach. We hope that our analysis may provide better insight into the origin of the reconstruction of the electronic spectrum observed in a recent experiment.[25] Note that our general approach for calculating the minimal conductivity can be applied to various other electronic systems.

Acknowledgments. We gratefully acknowledge fruitful discussions with K. S. Novoselov, V. P. Gusynin, and A. Pályi. This work was partially supported by the Hungarian Science Foundation OTKA under Contracts No. 75529 and No. 81492, by the Marie Curie ITN project NanoCTM (FP7-PEOPLE-ITN-2008-234970), by the European Union, and cofinanced by the European Social Fund (Grant Agreement No. TAMOP 4.2.1/B-09/1/KMR-2010-0003).

[1] K. S. Novoselov, A. K. Geim, S. V. Morozov, D. Jiang, Y. Zhang, S. V. Dubonos, I. V. Grigorieva, and A. A. Firsov, Science **306**, 666 (2004).
[2] Y. B. Zhang, Y.-W. Tan, H. L. Stormer, and P. Kim, Nature (London) **438**, 201 (2005).
[3] K. S. Novoselov, E. McCann, S. V. Morozov, V. I. Fal'ko, M. I. Katsnelson, U. Zeitler, D. Jiang, F. Schedin, and A. K. Geim, Nat. Phys. **2**, 177 (2006).
[4] E. McCann and V. I. Fal'ko, Phys. Rev. Lett. **96**, 086805 (2006).
[5] B. E. Feldman, J. Martin, and A. Yacoby, Nat. Phys. **5**, 889 (2009).
[6] X. Du, I. Skachko, F. Duerr, A. Luican, and E. Y. Andrei, Nature (London) **462**, 192 (2009).
[7] Y. Lemonik, I. L. Aleiner, C. Tőke, and V. I. Fal'ko, Phys. Rev. B **82**, 201408 (2010).
[8] F. Zhang, H. Min, M. Polini, and A. H. MacDonald, Phys. Rev. B **81**, 041402 (2010); F. Zhang, J. Jung, G. A. Fiete, Q. Niu, and A. H. MacDonald, Phys. Rev. Lett. **106**, 156801 (2011); F. Zhang and A. H. MacDonald, e-print arXiv:1107.4727v1 [cond-mat.str-el].
[9] O. Vafek and K. Yang, Phys. Rev. B **81**, 041401 (2010).
[10] R. Nandkishore and L. Levitov, Phys. Rev. B **82**, 115124 (2010).
[11] E. V. Gorbar, V. P. Gusynin, and V. A. Miransky, JETP Lett. **91**, 314 (2008); Phys. Rev. B **81**, 155451 (2010).
[12] K. Sun, H. Yao, E. Fradkin, and S. A. Kivelson, Phys. Rev. Lett. **103**, 046811 (2009).
[13] V. Oganesyan, S. A. Kivelson, and E. Fradkin, Phys. Rev. B **64**, 195109 (2001).
[14] M. Mucha-Kruczyński, I. L. Aleiner, and V. I. Fal'ko, Phys. Rev. B **84**, 041404 (2011).
[15] E. McCann, D. S. L. Abergel, and V. I. Fal'ko, Eur. Phys. J. Special Topics **148**, 91 (2007).
[16] J. Cserti, Phys. Rev. B **75**, 033405 (2007).
[17] I. Snyman and C. W. J. Beenakker, Phys. Rev. B **75**, 045322 (2007).
[18] K. Ziegler, Phys. Rev. B **75**, 233407 (2007).
[19] S. Ryu, C. Mudry, A. Furusaki, and A. W. W. Ludwig, Phys. Rev. B **75**, 205344 (2007).
[20] M. Trushin, J. Kailasvuori, J. Schliemann, and A. H. MacDonald, Phys. Rev. B **82**, 155308 (2010).
[21] D. Culcer and R. Winkler, Phys. Rev. B **79**, 165422 (2009).

[22] M. Koshino and T. Ando, Phys. Rev. B **73**, 245403 (2006).
[23] J. Cserti, A. Csordás, and G. Dávid, Phys. Rev. Lett. **99**, 066802 (2007).
[24] A. G. Moghaddam and M. Zareyan, Phys. Rev. B **79**, 073401 (2009).
[25] A. S. Mayorov, D. C. Elias, M. Mucha-Kruczyński, R. V. Gorbachev, T. Tudorovskiy, A. Zhukov, S. V. Morozov, M. I. Katsnelson, V. I. Falko, A. K. Geim, and K. S. Novoselov, Science **333**, 860 (2011).
[26] Y.-W. Son, S.-M. Choi, Y. P. Hong, S. Woo, and S.-H. Jhi, Phys. Rev. B **84**, 155410 (2011).
[27] See Supplemental Material at http://link.aps.org/supplemental/10.1103/PhysRevB.85.041402 for a discussion of the position of the Dirac points and the details of the calculations using the Landauer approach.
[28] M. I. Katsnelson, K. S. Novoselov, and A. K. Geim, Nat. Phys. **2**, 620 (2006).
[29] J. Tworzydło, B. Trauzettel, M. Titov, A. Rycerz, and C. W. J. Beenakker, Phys. Rev. Lett. **96**, 246802 (2006).
[30] R. A. Horn and C. R. Johnson, *Matrix Analysis* (Cambridge University Press, Cambridge, UK, 1985).
[31] H. U. Baranger and A. D. Stone, Phys. Rev. B **40**, 8169 (1989).